PCCP

ROYAL SOCIETY OF CHEMISTRY

PAPER

View Article Online
View Journal | View Issue

Check for updates

Cite this: *Phys. Chem. Chem. Phys.*, 2021, **23**, 17300

A theoretical insight into the curing mechanism of phthalonitrile resins promoted by aromatic amines†

Zuowei Chen, Liquan Wang, * Jiaping Lin * and Lei Du

Received 2nd May 2021,
Accepted 26th July 2021

DOI: 10.1039/d1cp01947c

rsc.li/pccp

High-temperature phthalonitrile resins have a wide range of applications, and understanding their curing mechanism is of great importance for academic research and engineering applications. However, the actual curing mechanism is still elusive. We presented a density functional theory study on the curing mechanism of phthalonitrile resins promoted by aromatic amines using phthalonitrile and aniline as the model compounds. We found that the rate-determining step is the initial nucleophilic addition of amines with nitrile groups on phthalonitrile to generate an amidine intermediate. The amines play a vital role in the H-transfer promoter throughout the curing reaction. The amidine and isoindoline are the critical intermediates, which can readily react with phthalonitrile through 6-membered transition states. The intramolecular cyclization of amidine intermediates is the vital step in forming isoindoline intermediates, which can be significantly promoted by amines. The proposed curing reaction pathways are kinetically more favorable than the previously reported ones, which can account for the formation of triazine, polyisoindoline, and phthalocyanine and provide a molecular-level understanding of the curing reaction.

Introduction

With the rapid development of aerospace industries, various high-performance polymers, such as epoxies, bismaleimides, and polyimides, have emerged to meet the harsh application conditions.[1–4] Among them, phthalonitrile-based resins demonstrate high thermal and oxidative stability, flame and moisture resistance, and excellent mechanical properties.[5–9] Those properties make the phthalonitrile resins attractive for a wide range of applications, such as aerospace, marine, and electronic packaging. A representative structure of phthalonitrile monomers is shown in Scheme 1a. The curing reaction of these resins occurs through nitrile groups by an addition mechanism, which results in void-free networks. The excellent properties of final cured resins can be attributed to the aromatic heterocyclic cross-links. Many research efforts have been devoted to characterizing the curing reaction of phthalonitrile resins to control the cross-linked structures and properties. However, the actual curing mechanism is still unclear.

One drawback of phthalonitrile resins is that the polymerization of neat phthalonitrile resins is exceptionally sluggish and requires several days at elevated temperatures, limiting the extensive industrial applications. It was found that the curing reaction can be promoted by curing agents, such as aromatic amines, phenolic compounds, metals and their salts, and coordination compounds.[10–13] Recently, self-promoted curing reaction of hydroxyl- or amino-containing phthalonitrile derivatives offers a new route to fabricating phthalonitrile resin.[14–17] It needs to point out that the phthalonitrile resins with metal curing agents have poor oxidative stability because of metal-catalyzed oxidation. In contrast, the nucleophilic compounds containing active hydrogens are suitable candidates as

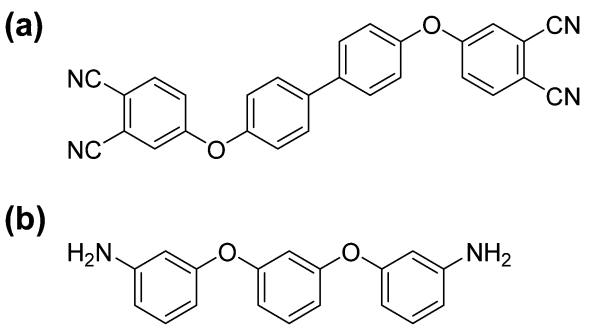

Scheme 1 Representative structures of (a) phthalonitrile monomer and (b) diamine curing agent.

Shanghai Key Laboratory of Advanced Polymeric Materials, Key Laboratory for Ultrafine Materials of Ministry of Education, Frontiers Science Center for Materiobiology and Dynamic Chemistry, School of Materials Science and Engineering, East China University of Science and Technology, Shanghai 200237, China. E-mail: lq_wang@ecust.edu.cn, jlin@ecust.edu.cn

† Electronic supplementary information (ESI) available. See DOI: 10.1039/d1cp01947c

curing agents of phthalonitrile resins. They generate reactive intermediates that react rapidly with excess phthalonitrile monomers. Aromatic diamines are found to be the most effective curing agents for phthalonitrile resins, which were reported intensely during the past few decades.[5,6,10,18–21] Representative structure of aromatic diamine is shown in Scheme 1b.

Another limitation is that the nature of the curing reaction is complex, and the products are uncontrollable. Various analytical techniques were used to elucidate the nature of the curing reaction promoted by active hydrogens. Keller *et al.* firstly used the aromatic diamines as curing agents to promote thermal curing reaction of phthalonitrile resins and speculated that the primary product is polyisoindoline since the phthalonitrile is known to react with amines to yield aminoisoindolines.[10,22] Further Fourier transform infrared spectroscopy study shows that the triazine and phthalocyanine may also form as the polymerization reaction proceeds.[18] Afterwards, Burchill found that the cured phthalonitrile resins are mainly composed of triazine as the cross-links and contain a trace of phthalocyanine when a low concentration of amine was used.[23]

The widely reported curing mechanism of phthalonitrile resins promoted by active hydrogens is presented in Scheme 2.[9,10,16,24] It was speculated that the reaction starts with the addition of a nucleophile containing active hydrogens to a nitrile group on phthalonitrile, generating an imino group that becomes a new nucleophilic site. Note that the nucleophilic addition on nitrile groups is a promising method to prepare a variety of useful organic compounds, which have been widely studied in both experimental and theoretical aspects.[25–28] Subsequently, the primary imine can nucleophilically attack the nitrile group on another phthalonitrile to form a dimer containing another primary imino group (Scheme 2, Pathway A). Further, a similar nucleophilic addition proceeds, following a series of cyclization and elimination, to form triazine cross-links. Alternatively, the nitrogen atom of the primary imino group can also attack the carbon atom of the adjacent nitrile group affording an isoindoline intermediate (Scheme 2, Pathway B). The primary imino group on isoindoline intermediates then reacts with the other phthalonitrile monomers to form phthalocyanine or polyisoindoline.

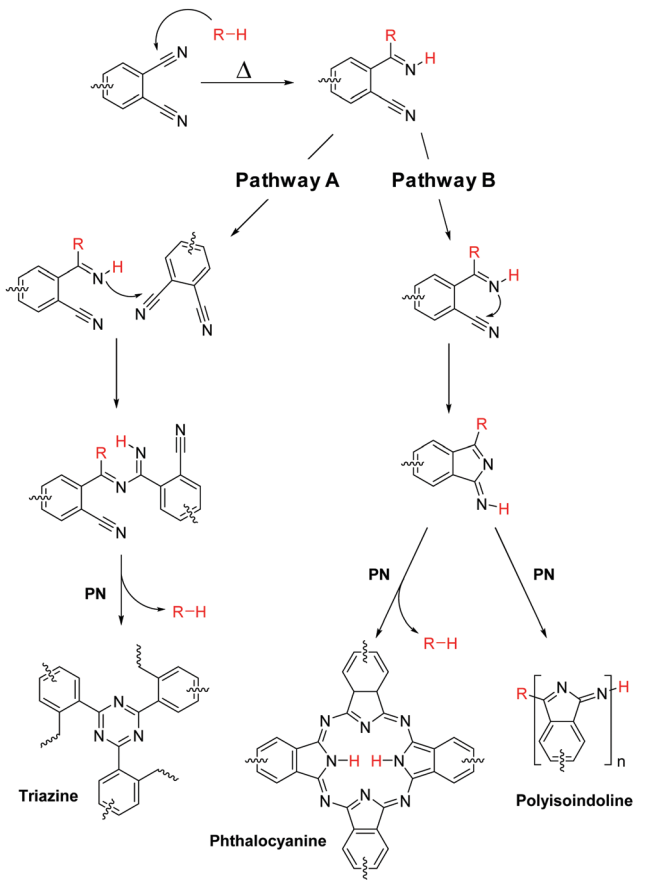

Scheme 2 Reported curing mechanism of phthalonitrile resins promoted by active hydrogens. **PN** represents the phthalonitrile monomer.

It is noteworthy that effort paid towards clarifying the curing mechanism of phthalonitrile resins seems to be limited to the preliminary exploration by experimental analysis techniques. Because the existing experimental techniques are usually difficult to characterize the reaction intermediates, it cannot provide information at the molecular level on the mechanism. The actual curing mechanism, including all elementary reactions, is still unclear. In addition, the reported curing mechanism shown in Scheme 2 cannot account for the experimental findings that a low concentration of aromatic amine promotes the curing reaction of phthalonitrile resins with the triazine as the major product.[23]

Because the overall properties of phthalonitrile resins depend on the cross-linked structures, a fundamental understanding of the curing mechanism is crucial for developing new polymer materials. In the present work, we explored the detailed energy surfaces of the possible reaction pathways using quantum chemical calculations, which have been demonstrated to be an efficient theoretical approach to reveal such complex curing mechanisms.[29–31] The work unravels the long-standing inconclusive curing mechanism of phthalonitrile resins, which can guide the control of the curing products and the development of the new high-temperature polymers.

Computational methodology

In this work, we employed the density functional theory method, which is a powerful approach in quantum chemistry calculations and has been successfully used in many fields of chemistry.[32] The calculations were performed using the density functional M06-2X with a D3 dispersion correction.[33,34] The M06-2X functional was chosen because it was shown to align with the experiment for organic structures. The structures of all reactants, products, intermediates and transition states were fully optimized with the 6-31G(d,p) basis set in the gas phase. The electronic energies of optimized structures were refined with the larger basis set of 6-311+G(d,p). Intrinsic reaction coordinate (IRC) calculations were also employed to confirm the identity of the reactants and products corresponding to

each transition state structure.[35,36] Normal mode analyses were performed with the same functional and basis set as the geometry optimizations. Thermal corrections to the molecular enthalpies (H_{corr}) and Gibbs free energies (G_{corr}) were computed based on the ideal gas approximation. Experimentally, a typical sample of phthalonitrile resins is cured by heating at 260 °C for 8 h, 280 °C for 8 h, and 315 °C for 8 h, and the post-curing is required to increase the cross-linking degree.[20] Therefore, we calculated the thermal contributions at 260 °C in this work. All calculations were carried out using the Gaussian 09 suite of programs.[37]

It is noteworthy that the curing reaction of phthalonitrile occurs in the condensed phase. The entropic contributions based on the ideal gas-phase model are often overestimated because it ignores the suppression effects of surrounding molecules on the translational and rotational freedoms of the reactants. As a result, the activation free energies for bimolecular reactions could be substantially overestimated due to the overestimated entropic decrease. However, the accurate calculation of activation entropies in the condensed phase is still a challenge for computation chemistry. Since no standard approach is currently available, diverse empirical correction methods have arisen to deal with the entropic problem.[38] One conventional approach considers that the entropy for each species in the condensed phase equals about half of its gas-phase entropy. This approach has been widely used to study a variety of reacting systems.[38–42] In this work, we followed this approach that the corrected free energy ($G_{50\%}$) is calculated by cut half of the corresponding gas-phase entropy (S_{gas}). Accordingly,

$$G_{gas} = E_{elec} + H_{corr} - TS_{gas} = E_{elec} + G_{corr} \quad (1)$$

$$G_{50\%} = E_{elec} + H_{corr} - \frac{1}{2}TS_{gas} = E_{elec} + \frac{1}{2}(H_{corr} + G_{corr}) \quad (2)$$

where G_{gas} is the uncorrected free energy in the gas phase, E_{elec} is the electronic energy. The corrected free energy $G_{50\%}$ is used in the following mechanistic discussion. The uncorrected free energies (G_{gas}) and enthalpies (H) based on the gas-phase calculations are given in the ESI.†

The obtained activation free energies were further used to calculate the intrinsic rate constants using the classical transition state theory (TST)[43]

$$k(T) = \kappa(T)\frac{k_B T}{h}\left(\frac{RT}{P^\circ}\right)^{\Delta n} e^{-\frac{\Delta G^\ddagger}{RT}} \quad (3)$$

where k_B is the Boltzmann constant, h is the Planck constant, R is the ideal gas constant, and P° is standard pressure (10^5 Pa). $\Delta G^\ddagger$ represents the molar Gibbs free energy of activation for the considered reaction at the standard gas state. Δn = 1 or 0 for bimolecular or unimolecular reaction, respectively. The quantum effects in the motion along the reaction path were considered using the Wigner tunneling correction[44]

$$\kappa(T) \approx 1 + \frac{1}{24}\left(\frac{h\nu^\ddagger}{k_B T}\right)^2 \quad (4)$$

where $\nu^\ddagger$ is the imaginary frequency of the transition state.

Results and discussion

For the sake of computational efficiency, we chose phthalonitrile and aniline, the simplest representatives of phthalonitrile-containing monomers and aromatic amines, respectively, as the compounds to study the curing reaction. Considering the previous experimental studies, we elucidated the reported curing mechanism (Scheme 2) and the other possible reaction pathways. Finally, the most probable reaction pathways are revealed. The corresponding transition state structures are given in the ESI.†

1. Nucleophilic addition of aniline to phthalonitrile

Generally, there are three types of mechanisms for the nucleophilic addition of primary amines to organic nitriles: associative, dissociative, and concerted. The associative mechanism starts with the nucleophilic attack of amine to the carbon atom of nitrile groups, giving a zwitterionic intermediate that may be converted into the final products *via* a proton transfer. However, in our computation, no intermediate of zwitterion was found in the nucleophilic addition of aniline to nitrile groups on the phthalonitrile. The associative mechanism was commonly found in the nucleophilic addition of metal-coordinated nitriles because the metals can stabilize the zwitterionic intermediate. In addition, the dissociative mechanism includes the initial deprotonation of nucleophiles, which usually needs any base from the reaction mixture, such as water and nucleophilic additives. This mechanism was found to be energetically demanding compared to the associative and concerted mechanisms.[28] Therefore, we only considered the concerted mechanism in this work.

The concerted mechanism involves forming a new C–N bond accompanied with simultaneous H-transfer from amino nitrogen to nitrile nitrogen in one step. This mechanism includes the generation of a transition state, which may be a 4-membered or 6-membered ring. In the latter case, the two aniline molecules are involved in the H-transfer, forming a 6-membered cyclic transition state. The aniline can attack the nitrile group *via* a transition state where the phenylamino group is *syn* or *anti* to the adjacent nitrile group (see Scheme 3). The free energy surfaces are shown in Fig. 1.

Although the *syn* transition state **TS1-2** seems more sterically crowded than the *anti*-**TS1-1**, the activation free energy (56.0 kcal mol^{-1}) of **TS1-2** is lower than that (61.0 kcal mol^{-1}) of **TS1-1**. It may be attributed to the stronger electrostatic attraction between the H atom on the phenylamino group and the N atom on the nitrile group (see Fig. S1 in the ESI,† **TS1-2**). However, the rate coefficient calculated by the TST method for the *syn* addition reaction is 9.5 × 10^{-9} L mol^{-1} s^{-1}

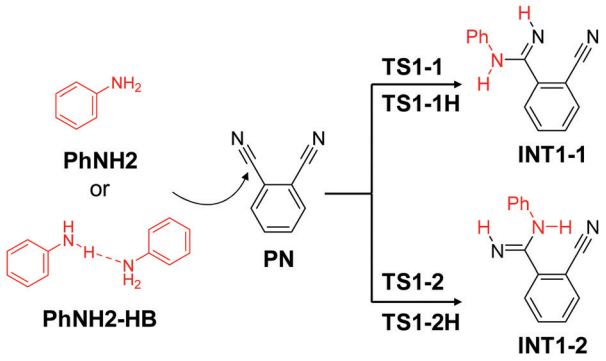

Scheme 3 Nucleophilic addition of aniline **PhNH2** or its hydrogen bonding complex **PhNH2-HB** to the nitrile group on phthalonitrile **PN**.

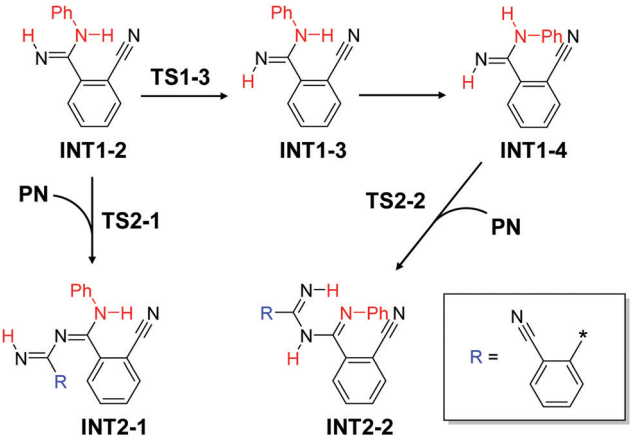

Scheme 4 Two possible reaction pathways from amidine intermediate **INT1-2**.

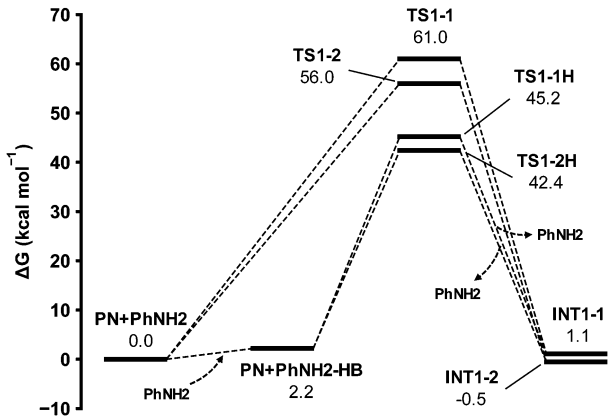

Fig. 1 Free energy surfaces of the nucleophilic addition of aniline **PhNH2** or its hydrogen bonding complex **PhNH2-HB** to the nitrile group on phthalonitrile **PN**.

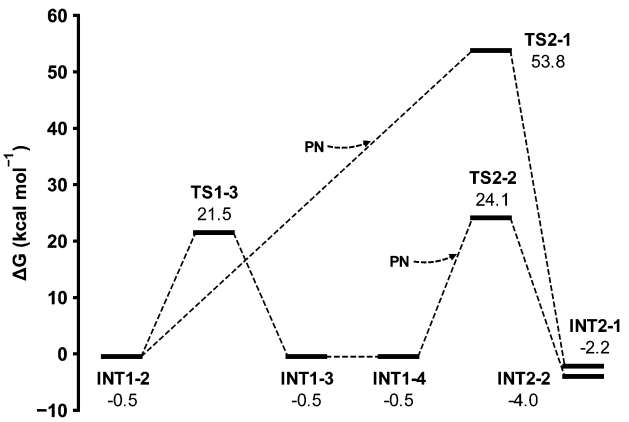

Fig. 2 Free energy surfaces of the reaction pathways from amidine intermediate **INT1-2**.

at 260 °C, which seems unacceptable to accomplish the reaction. As expected, the nucleophilic addition of aniline to phthalonitrile *via* a 6-membered cyclic transition state **TS1-1H** or **TS2-2H** (see Fig. S1 in the ESI†) is more energetically favorable than the pathway *via* a 4-membered cyclic transition state because of the higher stability of 6-membered structures. The activation free energies of **TS1-1H** and **TS1-2H** are 43.0 and 40.2 kcal mol^{-1}, and the calculated rate coefficients are 1.5×10^{-3} and 2.1×10^{-2} L mol^{-1} s^{-1}, respectively. The amidine intermediate **INT1-2** is 1.6 kcal mol^{-1} in free energy lower than **INT1-1**. Note that the nucleophilic addition assisted by the second aniline molecule requires the prior formation of the hydrogen bonding complex of anilines.

2. Reaction pathways for forming triazine from INT1-2

Since the amidine intermediate **INT1-2** is more energetically favorable than **INT1-1**, we first considered the reaction pathways starting from **INT1-2**. The possible reaction pathways from amidine intermediate **INT1-2** are shown in Scheme 4. Fig. 2 presents the free energy surfaces of these reaction pathways. According to the reported mechanism, the primary imino group of **INT1-2** is the new active nucleophilic site that can further attack the nitrile group *via* the transition state **TS2-1**, resulting in a dimer of phthalonitrile. Our computations show that it requires an activation free energy of 54.3 kcal mol^{-1}, comparable with that of the nucleophilic addition of a primary amine to phthalonitrile. The calculated rate coefficient is 4.6×10^{-8} L mol^{-1} s^{-1}. Therefore, this reaction pathway is excluded due to the unfavorable reaction rate.

In another pathway, the **INT1-2** firstly isomerizes to **INT1-3** through a hydrogen switching transition state **TS1-3**. The calculated rate coefficient of the isomerization is 1.5×10^{4} s^{-1}. It implies that the *cis-trans* isomerization of the N=C double bond proceeds quickly at the high reaction temperature of 260 °C. Thus, we neglected the transition state for the *cis-trans* isomerization of N=C double bonds in the discussion below for simplicity. The **INT1-3** then isomerizes to **INT1-4** *via* a C–N single bond rotation, which generally has a tiny activation barrier. Therefore, we also ignore the transition states for the conformation changes *via* a single bond rotation. The generated **INT1-4** then reacts with a phthalonitrile molecule by direct one-step addition of amidine structure to nitrile group *via* the

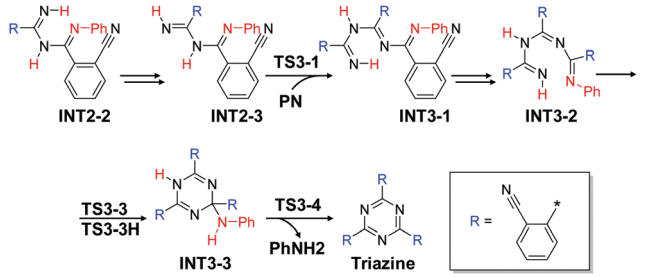

Scheme 5 Reaction pathways of the formation of triazine from amidine intermediate **INT2-2**.

transition state **TS2-2**, including the simultaneous formation of the C–N bond and H-transfer from the phenylamino group to the nitrile nitrogen. The activation free energy of **TS2-2** is 24.6 kcal mol^{-1}, and the calculated rate coefficient is 4.0×10^4 L mol^{-1} s^{-1}. It indicates that the reaction pathway of forming **INT2-2** is significantly faster than the nucleophilic addition of the primary imino group to nitrile *via* the transition state **TS2-1**, although the phthalonitrile dimer intermediate **INT2-2** is only 1.8 kcal mol^{-1} in free energy lower than **INT2-1**.

Along with the formation of the phthalonitrile dimer **INT2-2** discussed above, the **INT2-2** then proceeds similar reaction pathways of **INT1-2** and finally generates the cross-links of triazine, as shown in Scheme 5. The calculated free energy surfaces of these reaction pathways are presented in Fig. 3. Firstly, *cis–trans* isomerization and conformation transformation of **INT2-2** proceed to generate **INT2-3**. The amidine group of **INT2-3** attacks the nitrile group through the transition state **TS3-1** to form phthalonitrile trimer **INT3-1**. The activation free energy is 27.3 kcal mol^{-1}, slightly higher than that (24.6 kcal mol^{-1}) of the **TS2-2**. The calculated rate coefficient is 3.2×10^3 L mol^{-1} s^{-1}. A series of isomerization subsequently transforms the **INT3-1** to **INT3-2**. Further intramolecular cyclization, accompanied by the H-transfer from imino group to phenylimino nitrogen of **INT3-2**, occurs to generate cyclic intermediate **INT3-3**. This monomolecular reaction requires an activation free energy of 37.4 kcal mol^{-1}, under which the calculated rate coefficient is 7.0×10^{-3} s^{-1}.

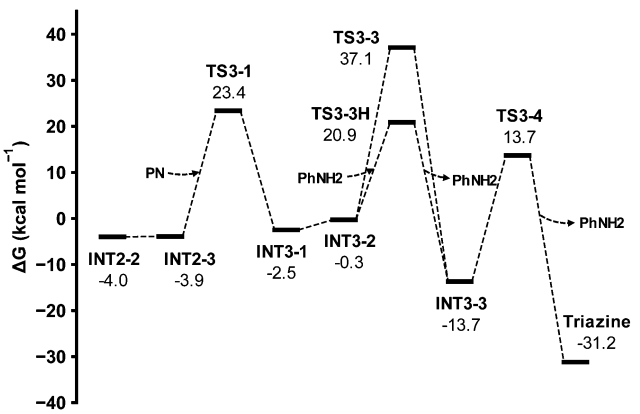

Fig. 3 Free energy surfaces of the formation of triazine from amidine intermediate **INT2-2**.

With the assistance of the second aniline molecule, the intramolecular cyclization can be significantly accelerated through the transition state **TS3-3H**. The calculated rate coefficient is 1.4×10^6 L mol^{-1} s^{-1} that is three orders of magnitude higher than that of the nucleophilic addition of **INT2-3** with phthalonitrile to give **INT3-1**. We assumed that the further addition reaction with phthalonitrile starting from **INT3-1** is similar to the reaction of **INT2-2** to form **INT3-1**. Therefore, the computational results indicate that phthalonitrile trimer **INT3-1** is more prone to intramolecular cyclization than nucleophilic addition with phthalonitrile. The cyclic intermediate **INT3-3** finally eliminates an aniline molecule *via* the transition state **TS3-4**, rapidly forming a triazine with the activation free energy of 27.4 kcal mol^{-1}. The calculated rate coefficient is 1×10^2 s^{-1}.

3. Reaction pathways for forming polyisoindoline and phthalocyanine from INT1-1

Scheme 6 presents the reaction pathways starting from amidine intermediate **INT1-1**. Our computation involves four possible reaction pathways. The calculated free energy surfaces of these reaction pathways are shown in Fig. 4. According to the reported mechanism, the **INT1-1** can transform to isoindoline intermediate **INT1-5** by an intramolecular cyclization *via* the transition state **TS1-5**. The intramolecular cyclization of **INT1-1** has an exergonicity of 9.0 kcal mol^{-1}, which indicates that the isoindoline intermediate is more energetically favorable than the amidine intermediate. However, the activation free energy is 56.7 kcal mol^{-1}, which seems too high to overcome under the reaction temperature of 260 °C, and the calculated rate coefficient is only 1.2×10^{-10} s^{-1}.

In the reaction pathway through the transition state **TS1-5H**, the aniline molecule acts as an H-transfer shuttle to prompt the formation of isoindoline intermediate **INT1-5**. The required activation free energy is significantly reduced to 27.0 kcal mol^{-1} because of the lower bending energy of the C=N–H fragment in the **TS1-5H** compared to that in the **TS1-5**, and the calculated rate coefficient is 6.0×10^3 L mol^{-1} s^{-1}. It indicates that the cyclization of amidine intermediate **INT1-1** may greatly depend on the amine concentration. We found that the phthalonitrile can also promote the formation of isoindoline. In this competitive pathway, the H atom of primary imino groups and the N atom of adjacent nitrile groups on the **INT1-1** attack the phthalonitrile to form intermediate **INT2-4** *via* the transition state **TS2-4**. It requires an activation free energy of 37.2 kcal mol^{-1}, and the rate coefficient is 2.9×10^{-1} L mol^{-1} s^{-1}, which is four orders of magnitude lower than the rate coefficient of the reaction pathway through **TS1-5H**. Because the amount of curing agents is usually in the range of 1.5–2% by the weight of the phthalonitrile monomers, it is more favorable to form the isoindoline promoted by amines.

The primary imino group on isoindoline intermediate **INT1-5** then becomes a new nucleophilic site, which can react with phthalonitrile through two pathways. The direct nucleophilic addition of the imino group to nitrile is unfavorable since its activation free energy (58.7 kcal mol^{-1}) is too high. In another pathway, the intermediate **INT1-5** nucleophilically attacks a

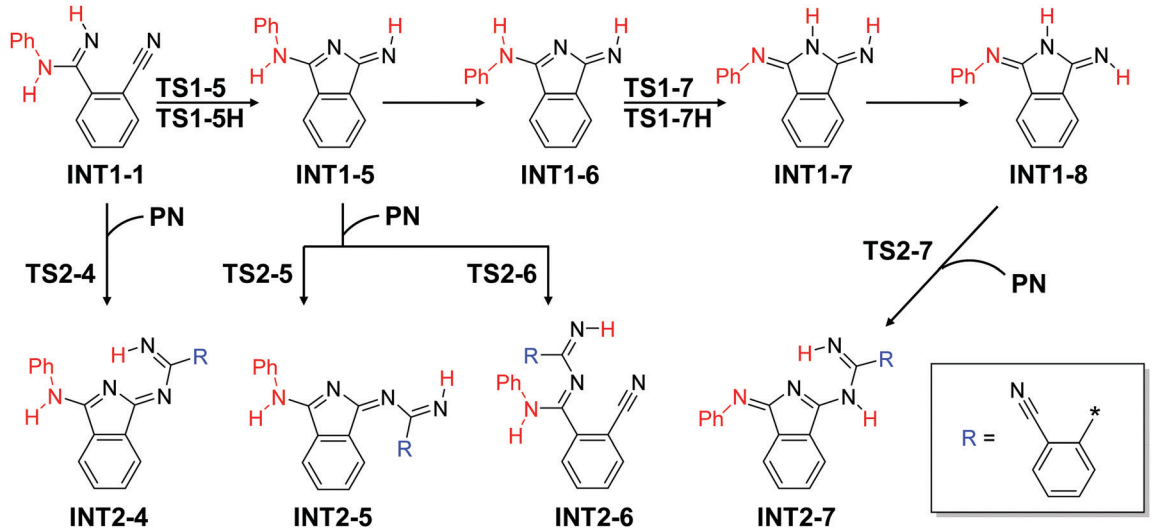

Scheme 6 Possible reaction pathways from amidine intermediate **INT1-1**.

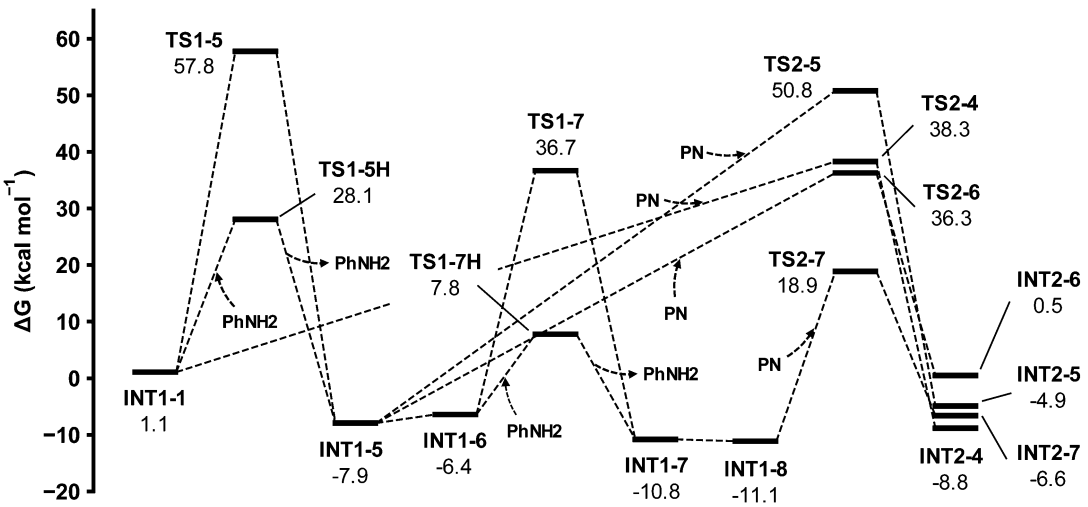

Fig. 4 Free energy surfaces of the reaction pathways from amidine intermediate **INT1-1**.

phthalonitrile, accompanied by a ring-opening of isoindoline. Because of the stability of the 6-membered structure of **TS2-6**, the activation free energy (44.2 kcal mol^{-1}) is reduced relative to that of the pathway through **TS2-5**. However, the activation free energy is still too high to be overcome since the calculated rate coefficient (5.1×10^{-4} L mol^{-1} s^{-1}) is small.

According to our computational results, the amidine intermediate **INT1-5** can transform to the other isomers. Firstly, a single bond rotation changes the **INT1-5** to **INT1-6**. The **INT1-6** has a tautomeric form **INT1-7**, which can transform each other through an intramolecular H-transfer. The direct intramolecular H-transfer converts the **INT1-6** to **INT1-7** with an activation free energy of 43.1 kcal mol^{-1} and a rate coefficient of 5.1×10^{-5} s^{-1}. The help of amines can reduce the activation free energy to 14.2 kcal mol^{-1} and increases the rate coefficient to 8.4×10^{8} L mol^{-1} s^{-1}. The tautomeric form **INT1-7** is more favorable in free energy than **INT1-6**, as shown in Fig. 4. Subsequent hydrogen switch further converts the **INT1-7** to **INT1-8**. The generated **INT1-8** then reacts with a phthalonitrile *via* the 6-membered cyclic transition state **TS2-7** with an activation free energy of 30.0 kcal mol^{-1}. The calculated rate coefficient is 2.7×10^{2} L mol^{-1} s^{-1}. As shown in Fig. 4, the activation free energy from **INT1-5** to **TS2-6** is 44.2 kcal mol^{-1} higher than that from **INT1-8** to **TS2-7**. This difference can be attributed to the isoindoline cyclic structure, which is more energetically favored than the amidine mentioned above and is opened in the reaction from **INT1-5** to **INT2-6**.

Along with the formation of the phthalonitrile dimer **INT2-7** in the preceding step, a series of elementary reactions lead to the phthalonitrile trimer **INT3-5** (see Scheme 7). These reaction processes are similar to the pathway from **INT1-1** to **INT2-7** (see Scheme 6). The detailed free energy surfaces are

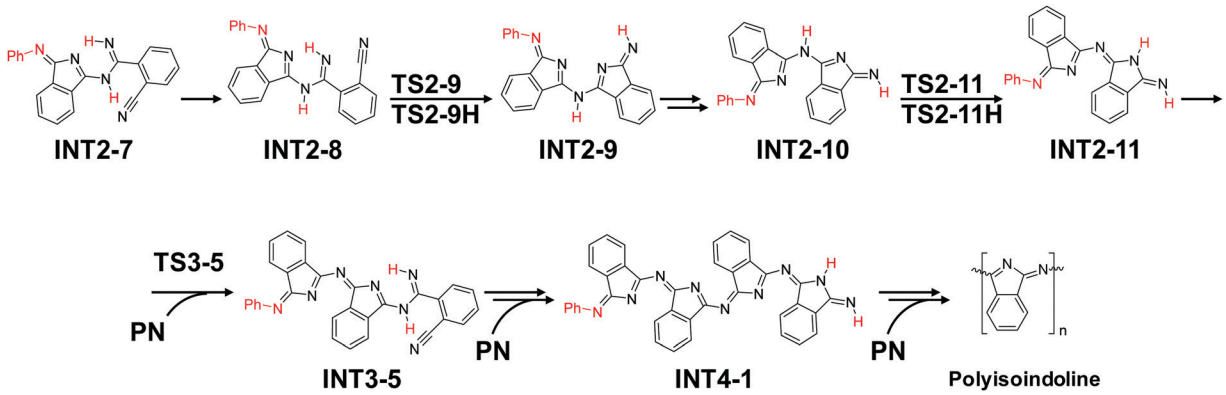

Scheme 7 Reaction pathways for forming polyisoindoline from amidine intermediate **INT2-7**.

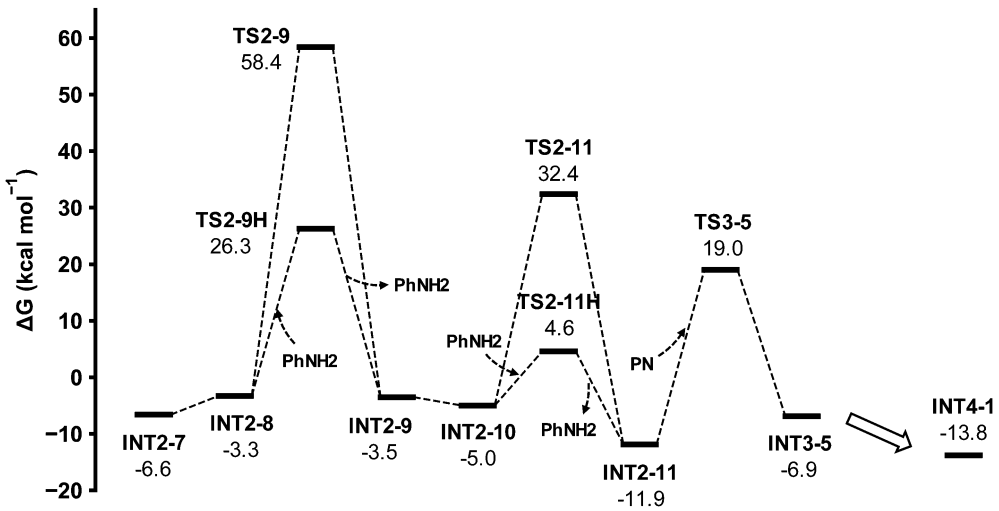

Fig. 5 Free energy surfaces for forming phthalonitrile tetramer **INT4-1** from amidine intermediate **INT2-7**.

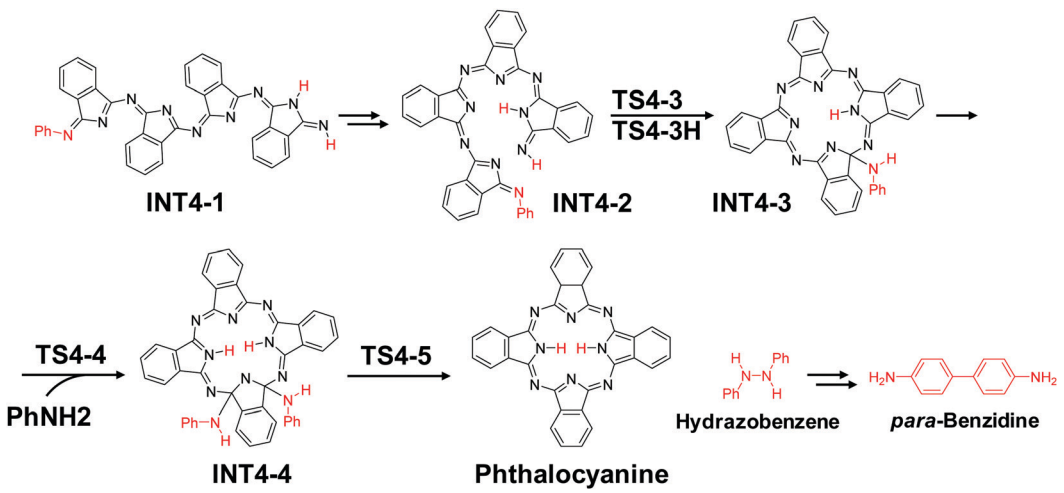

Scheme 8 Reaction pathways for forming phthalocyanine from amidine intermediate **INT4-1**.

shown in Fig. 5. Note that the further reaction of phthalonitrile trimer **INT3-5** with phthalonitrile to give tetramer **INT4-1** was assumed to be similar to the reaction from **INT2-7**, and therefore the free energy surfaces are not shown in Fig. 5. After the formation of **INT4-1**, two reaction pathways might be involved. One is that the nucleophilic addition of **INT4-1** to

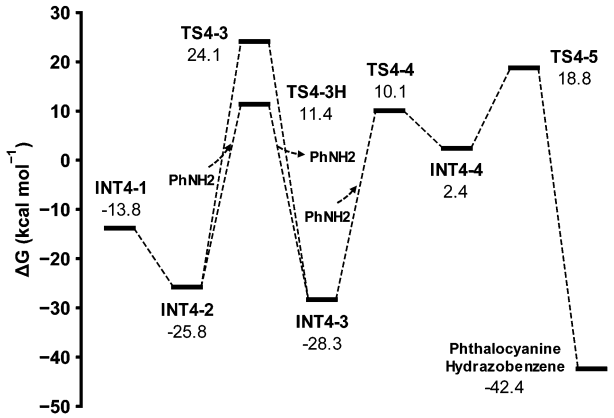

Fig. 6 Free energy surfaces for forming phthalocyanine from amidine intermediate **INT4-1**.

phthalonitrile further generates the polyisoindoline product as found in experiments (see Scheme 7).

Another reaction pathway shown in Scheme 8 is that **INT4-1** firstly isomerizes to **INT4-2** *via* a series of *cis-trans* isomerization and single bond rotation. The free energy surfaces are presented in Fig. 6. The overall isomerization is significantly exergonic by 12.0 kcal mol^{-1}, which indicates that **INT4-2** is more favorable than **INT4-1**. In the subsequent elementary reaction, the ring-closure of **INT4-2** proceeds *via* the transition state **TS4-3** with an activation free energy of 49.9 kcal mol^{-1}, and the calculated rate coefficient is only 5.1×10^{-8} s^{-1}. With the assistance of amines, the activation free energy can decrease to 37.2 kcal mol^{-1}, and the calculated rate coefficient is 7.1×10^{-1} L mol^{-1} s^{-1}. Note that the intramolecular cyclization of phthalonitrile tetramer **INT4-2** is much slower than that of the phthalonitrile trimer **INT3-2** to form the triazine cross-link even under amine-assisted conditions.

Directly eliminating the aniline from intermediate **INT4-3** is not favored as this would lead to the dehydrophthalocyanine, a highly unstable 16π-electron system. We, therefore, suggested that the second molecule of aniline could participate in the elimination to give 18π-electron aromatic phthalocyanine product and leave a hydrazobenzene molecule, as shown in Scheme 8. The amine could attack the intermediate **INT4-3** to form **INT4-4**. This process has an activation free energy of 38.4 kcal mol^{-1} and a rate coefficient of 1.1×10^{-1} L mol^{-1} s^{-1}. Subsequently, the **INT4-4** eliminates a hydrazobenzene molecule with an activation free energy of 16.4 kcal mol^{-1}. The calculated rate coefficient is 2.2×10^{6} s^{-1}. The hydrazobenzene compound is unstable and could rearrange to other products such as benzidine, diphenyline, and semidine. This rearrangement is the so-called "benzidine rearrangement", which refers to a class of rearrangements of hydrazo aromatics, and has been widely studied.[45–47] It has been found that the reaction that includes the rearrangement of hydrazobenzene yields *para*-benzidine as the main product. Consequently, the generated primary amino group on *para*-benzidine further promotes the curing of phthalonitrile resins.

The detailed curing mechanism of phthalonitrile resins can be elucidated by summarizing the above results. Based on the previously reported mechanism shown in Scheme 2, we proposed kinetically more favorable reaction pathways summarized in Scheme 9. The computations suggest that the direct nucleophilic addition of amine or imino groups to nitriles *via* 4-membered transition states and the intramolecular cyclization of amidine to isoindoline intermediates are too slow to proceed under the curing conditions reported in the literature. In contrast, we found those reactions can be significantly promoted by the amines as the H-transfer shuttle. Furthermore, the amidine intermediates can react with phthalonitrile through a 6-membered cyclic transition state like **TS2-2**, and further similar nucleophilic addition with phthalonitrile

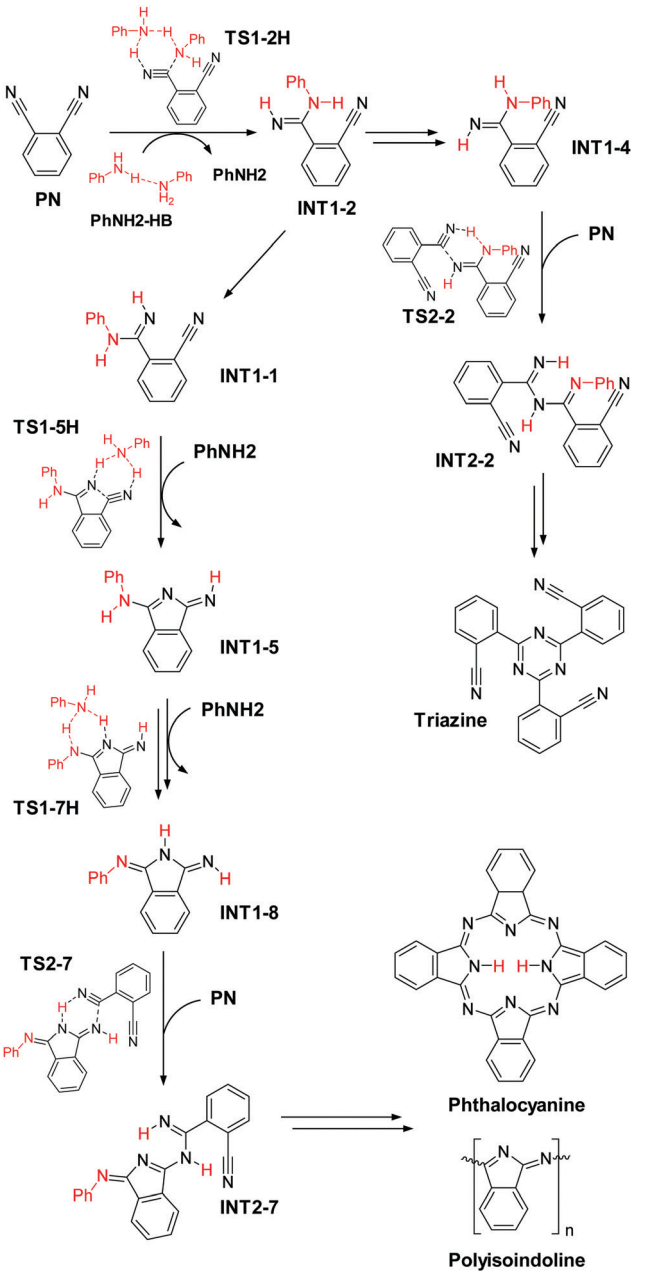

Scheme 9 Summary of the favorable curing reaction pathways of phthalonitrile resins promoted by amines.

proceeds to finally produce the triazine product. The intramolecular cyclization of amidine intermediates requires the promotion of amines to generate isoindoline intermediates. A series of isomerization then transform the isoindoline intermediate to its tautomeric form that can more readily react with phthalonitrile through a 6-membered cyclic transition state like **TS2-7** and finally give polyisoindoline or phthalocyanine product.

It is worth mentioning that the amidine and isoindoline intermediates are critical to the composition of cured products. As can be seen, at the low amine concentration, the amidine intermediates are favored to attack the phthalonitrile monomers nucleophilically and finally produce the triazine product, rather than to generate isoindoline intermediates *via* intramolecular cyclization. As a result, the primary product is triazine when small amounts of amines are added, which agrees with the experimental findings reported by Burchill.[23] The experiment results show that a highly cross-linked polytriazine was obtained when 4,4′-bis(3,4-dicyanophenoxy)biphenyl is heated with small amounts of aromatic amine or amidine salts. However, the previously reported mechanism cannot account for the experimental findings because the occurring ratio of reaction pathways A and B shown in Scheme 2 are independent of amine concentration. In short, our proposed reaction pathways are more kinetically favorable than the reported ones and can explain the formation of curing products observed in experiments.

Finally, we want to emphasize that the proposed curing mechanism is of value in developing the new phthalonitrile resins. It is known that the high thermal stability mainly comes from the heteroaromatic cross-links, including triazine and phthalocyanine.[16] This work provides an insight into the curing reaction, which helps to control the final product composition and further develop the phthalonitrile resins with higher thermal stability. For instance, the proportion of triazine products can be tuned by controlling the concentration of amines. In addition, the curing temperature of phthalonitrile resins is also essential for resin processing. The work indicates that the rate-determining step is the initial nucleophilic addition of amine with nitrile groups on phthalonitrile, which can be significantly accelerated by forming the hydrogen bonding complex of amines. This computational result can be used to estimate the reactivity of amines to nitrile groups, which helps the molecular design of more effective amine curing agents.

Notably, the work is focused on the energy surfaces of reaction pathways to account for the formation of various curing products. The overall curing reaction of phthalonitrile resins is complex, involving multiple unimolecular and bimolecular reaction steps. Because the higher temperature and lower reactant concentration favor the unimolecular reaction over the bimolecular reaction due to entropic reasons, the curing conditions such as the amount of reactants and reaction temperatures could significantly affect the final products. Therefore, a detailed kinetic analysis is desired to obtain the quantitative composition of final products. However, the complexity of the curing reaction makes the kinetic modeling difficult. In addition, it is a challenge to consider the effect of diffusion in kinetic modeling as it is incapable of being studied using DFT methods. Nevertheless, the exploration of the energy surface of curing reactions can enable establishing a complete kinetic model for the curing process in the future.

Conclusions

We presented a comprehensive study on the thermal curing mechanism of phthalonitrile resins promoted by aromatic amines using density functional theory methods. The model compounds of phthalonitrile and aniline were used in this work. The computational results revealed that the rate-determining step is the initial nucleophilic addition of amine with nitrile groups on phthalonitrile to generate an amidine intermediate. We found that the amines play a vital role in the H-transfer promoter throughout the curing reaction. In addition, the amidine and isoindoline are the critical intermediates. They can both readily react with phthalonitrile *via* 6-membered transition states. The intramolecular cyclization of amidine to form isoindoline requires the assistance of amines. Accordingly, the amidine intermediate is more favored to react with another phthalonitrile molecule than the intramolecular cyclization at the low amine concentration. The direct intramolecular cyclization of amidine to isoindoline without the assistance of amines and the nucleophilic addition of imino groups on the amidine or isoindoline intermediates to phthalonitrile *via* 4-membered transition states are too slow to proceed under the typical experimental conditions. The proposed curing reaction pathways are kinetically more favorable than the reported ones in the literature and can reasonably account for the formation of triazine, polyisoindoline, and phthalocyanine, which help develop new high-temperature phthalonitrile resins.

Conflicts of interest

There are no conflicts to declare.

Acknowledgements

This work was supported by the National Natural Science Foundation of China (51833003, 21774032, 51621002, and 21975073).

References

1 P. M. Hergenrother, *High Perform. Polym.*, 2003, **15**, 3–45.
2 D.-J. Liaw, K.-L. Wang, Y.-C. Huang, K.-R. Lee, J.-Y. Lai and C.-S. Ha, *Prog. Polym. Sci.*, 2012, **37**, 907–974.
3 G. Gao, S. Zhang, L. Wang, J. Lin, H. Qi, J. Zhu, L. Du and M. Chu, *ACS Appl. Mater. Interfaces*, 2020, **12**, 27587–27597.
4 J. Zhu, M. Chu, Z. Chen, L. Wang, J. Lin and L. Du, *Chem. Mater.*, 2020, **32**, 4527–4535.
5 T. M. Keller and D. D. Dominguez, *Polymer*, 2005, **46**, 4614–4618.

6 M. Laskoski, D. D. Dominguez and T. M. Keller, *J. Polym. Sci., Part A: Polym. Chem.*, 2005, **43**, 4136–4143.
7 K. Zeng and G. Yang, *Wiley Encycl. Compos.*, 2011, 1–14.
8 M. Wang and Y. Ning, *ACS Appl. Mater. Interfaces*, 2018, **10**, 11933–11940.
9 G. Wang, Y. Han, Y. Guo, S. Wang, J. Sun, H. Zhou and T. Zhao, *Ind. Eng. Chem. Res.*, 2019, **58**, 9921–9930.
10 T. M. Keller and T. R. Price, *J. Macromol. Sci., Chem.*, 1982, **18**, 931–937.
11 M. Sumner, M. Sankarapandian, J. McGrath, J. Riffle and U. Sorathia, *Polymer*, 2002, **43**, 5069–5076.
12 N. B. McKeown, *J. Mater. Chem.*, 2000, **10**, 1979–1995.
13 K. Jia, R. Zhao, J. Zhong and X. Liu, *J. Mater. Sci.: Mater. Electron.*, 2010, **21**, 708–712.
14 K. Zeng, K. Zhou, S. Zhou, H. Hong, H. Zhou, Y. Wang, P. Miao and G. Yang, *Eur. Polym. J.*, 2009, **45**, 1328–1335.
15 H. Zhou, A. Badashah, Z. Luo, F. Liu and T. Zhao, *Polym. Adv. Technol.*, 2011, **22**, 1459–1465.
16 D. Augustine, D. Mathew and C. R. Nair, *Polym. Int.*, 2013, **62**, 1068–1076.
17 A. Badshah, M. R. Kessler, Z. Heng, J. H. Zaidi, S. Hameed and A. Hasan, *Polym. Chem.*, 2013, **4**, 3617–3622.
18 T. M. Keller, *J. Polym. Sci., Part A: Polym. Chem.*, 1988, **26**, 3199–3212.
19 S. B. Sastri, J. P. Armistead and T. M. Keller, *Polym. Compos.*, 1996, **17**, 816–822.
20 S. B. Sastri and T. M. Keller, *J. Polym. Sci., Part A: Polym. Chem.*, 1998, **36**, 1885–1890.
21 S. B. Sastri and T. M. Keller, *J. Polym. Sci., Part A: Polym. Chem.*, 1999, **37**, 2105–2111.
22 W. O. Siegl, *J. Org. Chem.*, 1977, **42**, 1872–1878.
23 P. Burchill, *J. Polym. Sci., Part A: Polym. Chem.*, 1994, **32**, 1–8.
24 J. Hu, Y. Liu, Y. Jiao, S. Ji, R. Sun, P. Yuan, K. Zeng, X. Pu and G. Yang, *RSC Adv.*, 2015, **5**, 16199–16206.
25 M. Kuznetsov, N. Bokach, V. Y. Kukushkin and A. Dement'ev, *Russ. J. Gen. Chem.*, 2009, **79**, 232–241.
26 M. Kuznetsov, N. Bokach, D. Kharlampidi, Y. N. Medvedev, V. Y. Kukushkin and A. Dementiev, *Russ. J. Gen. Chem.*, 2010, **80**, 458–467.
27 F. Tordini, A. Bencini, M. Bruschi, L. De Gioia, G. Zampella and P. Fantucci, *J. Phys. Chem. A*, 2003, **107**, 1188–1196.
28 J. Lasri, M. L. Kuznetsov, M. F. T. C. Guedes da Silva and A. J. Pombeiro, *Inorg. Chem.*, 2012, **51**, 10774–10786.
29 J.-E. Ehlers, N. G. Rondan, L. K. Huynh, H. Pham, M. Marks and T. N. Truong, *Macromolecules*, 2007, **40**, 4370–4377.
30 S. Kunnikuruvan, P. V. Parandekar, O. Prakash, T. K. Tsotsis and N. N. Nair, *Macromolecules*, 2017, **50**, 6081–6087.
31 Z. Chen, L. Wang, J. Lin and L. Du, *Phys. Chem. Chem. Phys.*, 2020, **22**, 6468–6477.
32 A. J. Cohen, P. Mori-Sánchez and W. Yang, *Chem. Rev.*, 2012, **112**, 289–320.
33 Y. Zhao and D. G. Truhlar, *Theor. Chem. Acc.*, 2008, **120**, 215–241.
34 S. Grimme, J. Antony, S. Ehrlich and H. Krieg, *J. Chem. Phys.*, 2010, **132**, 154104.
35 K. Fukui, *J. Phys. Chem.*, 1970, **74**, 4161–4163.
36 C. Gonzalez and H. B. Schlegel, *J. Chem. Phys.*, 1989, **90**, 2154–2161.
37 M. J. Frisch, G. W. Trucks and H. B. Schlegel, *et al.*, *Gaussian 09, Revision C.01*, Gaussian, Inc., Wallingford CT, 2010.
38 R. E. Plata and D. A. Singleton, *J. Am. Chem. Soc.*, 2015, **137**, 3811–3826.
39 L. Zhao, M. Wen and Z. X. Wang, Eur, *J. Org. Chem.*, 2012, 3587–3597.
40 J. Kua, A. A. Rodriguez, L. A. Marucci, M. M. Galloway and D. O. De Haan, *J. Phys. Chem. A*, 2015, **119**, 2122–2131.
41 J. K.-C. Lau and D. V. Deubel, *J. Chem. Theory Comput.*, 2006, **2**, 103–106.
42 F. Huang, G. Lu, L. Zhao, H. Li and Z.-X. Wang, *J. Am. Chem. Soc.*, 2010, **132**, 12388–12396.
43 H. Eyring, *J. Chem. Phys.*, 1935, **3**, 107–115.
44 E. Wigner, *J. Chem. Phys.*, 1937, **5**, 720–725.
45 H. Shine and J. Trisler, *J. Am. Chem. Soc.*, 1960, **82**, 4054–4058.
46 H. J. Shine, H. Zmuda, K. H. Park, H. Kwart, A. G. Horgan, C. Collins and B. E. Maxwell, *J. Am. Chem. Soc.*, 1981, **103**, 955–956.
47 M. E. Bouillon and H. H. Meyer, *Tetrahedron*, 2016, **72**, 3151–3161.